ASTRONOMY & ASTROPHYSICS
SUPPLEMENT SERIES

Astron. Astrophys. Suppl. Ser. **127,** 153-165 (1998)

Pulse shapes of radio pulsars at 4.85 GHz

J. Kijak[1,2], M. Kramer[1], R. Wielebinski[1], and A. Jessner[1]

[1] Max-Planck-Institut für Radioastronomie, Auf dem Hügel 69, D-53121 Bonn, Germany
[2] Astronomy Centre, Pedagogical University, Lubuska 2, PL-65-265 Zielona Góra, Poland

Received 27 March; accepted 25 April, 1997

Abstract. We present pulse shapes of 87 pulsars at 4.85 GHz. Pulse widths and flux densities are measured. The frequency dependence of the profile shape and the pulse width is discussed. Our data base has been combined with other published data to generate flux spectra between 1.4 GHz and 5 GHz. The mean flux spectral index has a value −1.9. Our analysis shows that pulsar emission spectra are steeper at higher frequencies.

Key words: pulsars: general — radiation mechanisms: miscellaneous

1. Introduction

Observations of integrated pulse profiles over a wide frequency range are important for an understanding of many aspects of radio pulsars. Mean pulse profiles of pulsars exhibit great stability but there are large morphological differences from pulsar to pulsar (Backer 1976; Morris et al. 1981; Rankin 1983; Lyne & Manchester 1988; Seiradakis et al. 1995). This fact has become the basis for a classification system first proposed by Huguenin et al. (1971) and finally developed by Rankin (1983). The morphological characteristics of observed pulse shapes provide us information on both the geometry and the mechanism of pulsar radiation. In the hollow-cone beam model for pulsar radio emission (Sturrock 1971; Ruderman & Sutherland 1975) the observed pulse shapes represent cuts across the radiated beam. Most pulsars show considerable changes of pulse shape and profile width with frequency. Simple profiles at low frequency are often resolved into several components at higher frequencies (Kramer 1994). These differences are partly due to the various ways in which the line of sight cuts across the radiated beam and partly due to the intrinsic asymmetries or irregulaties within the actual pulsar beams. The narrowing of profiles with increasing frequency is compatible with the hollow-cone model and supports the concept of a radius-to-frequency mapping (Cordes 1978).

Dispersion smearing and in particular, scatter broadening prohibit the detection of pulsars with high dispersion measures at low frequencies. However, the general steepness of pulsar spectra demands a highly sensitive observing system at high frequencies. The flux density of observed pulsars is known to be frequency dependent at lower frequencies with an average power-law index of −1.6 (Lorimer et al. 1995).

The profile morphology develops with increasing frequency either from a simple to a multiple component structure or vice versa. A classification scheme based on this fact (Rankin 1983) distinguishes between core and cone dominated profiles, depending on the radiating part of the emission cone. The so-called core component is identified with a central component of the pulse profile, which shows no drift in the corresponding sub-pulses. In contrast, cone components generally located at the outer edges of the pulse profiles, often exhibit drifting subpulses. In the hollow-cone model, the mean pulsar beam consists of a multiple cone structure nested around a core component located at the magnetic axis. This model describes simple and complex structures of pulse profiles well (Oster & Sieber 1976; Gil & Krawczyk 1997). In general, a core component is observed mainly at low frequencies and fades progressively towards higher frequencies. At the same time "conal outriders" become the dominant features in pulse profiles at high frequencies. This can be explained by geometrical effects (Kramer et al. 1994; Sieber 1997). Several studies present arguments for the multiconal beam structure which is implied by average pulsar profiles (Gil et al. 1993; Rankin 1993; Kramer et al. 1994; Gil & Krawczyk 1996). However, Lyne & Manchester (1988) claim that the components in the mean profile correspond to patchy beams fixed to the neutron star surface.

Nevertheless, both models assume that integrated profiles represent a true "long exposed" image of the radio beam. Thus, the study of flux densities, pulse widths and pulse shapes over a wide frequency range are very important for the understanding of the radio emission

Send offprint requests to: jkijak@astro.ca.wsp.zgora.pl

Table 2. Pulsars not detected at 4.85 GHz. The pulsar name, number of observations, total observing time and upper limits $S_{\max}$ for the flux density are listed

PSR B	N	Time [min]	$S_{\max}$ [mJy]	PSR B	N	Time [min]	$S_{\max}$ [mJy]
0320+39	1	30	0.03	1732−07	1	10	0.04
0353+52	1	15	0.06	1754−24	2	31	0.04
0410+69	2	30	0.02	1811+40	1	30	0.04
0531+21	3	40	0.02	1820−14	2	20	0.02
0613−02	1	10		1834−04	1	15	0.04
0621−04	3	41	0.01	1848+04	1	10	
0751+18	1	35		1848+12	1	10	0.04
0841+80	1	10		1859+01	1	25	0.03
1322+83	2	30	0.05	2044+15	3	50	0.03
1534+12	3	31		2229+26	1	15	
1700−18	1	20	0.03				

properties of pulsars. Therefore we have started a project to collect pulse shapes and flux densities in the widest range of frequencies possible. Up to now, 64 different pulsar profiles have been observed and presented at a wavelength of λ 6 cm using the 100-m radio telescope of the Max-Planck-Institut für Radioastronomie (see Sieber et al. 1975; Kuzmin et al. 1986; Izvekova et al. 1994; Seiradakis et al. 1995). In this paper we present a further 87 pulse shapes at 4.85 GHz. We have measured pulse widths at a level of 50 and 10 per cent of the pulse peak as well as mean flux densities (see Table 1). The results are used to discuss the profile development and the narrowing of pulse widths with frequency. The new data are combined with data from the literature to make a statistical study of the spectral behaviour of flux density.

2. Observations

Observations were performed between August 1995 and March 1996 at 4.85 GHz using the Effelsberg 100-m radio telescope. This survey aimed at weak pulsars ($S <$ 0.5 mJy) which were not observed during the last survey (see Seiradakis et al. 1995).

We used a new sensitive HEMT system at 4.85 GHz recently installed at the 100-m radio telescope. The system with a maximum bandwidth of 500 MHz has a system temperature of $T_{\rm sys} \lesssim 30$ K for elevations above 20°. We used either 4 channels of a 8×60 MHz filter bank as a de-disperser for two circular polarizations or broad-band signals with 500 MHz bandwidth or a narrow-band polarimeter with a bandwidth of $80 - 200$ MHz for full polarimetry observations (see Hoensbroech et al. in preparation). The filter bank was used in order to reduce the dispersion broadening for pulsars where the effect was significant (larger than $P/1024$, where P is the pulsar period), in particular for objects with a high DM. A detailed description of the observing system and the calibration procedure can be found in Seiradakis et al. (1995) and Kramer et al. (1996).

During about 80 hours of total observing time we observed 108 pulsars. The average integration time for detecting a pulsar was about $10 - 15$ minutes.

3. Results

From our sample of 108 pulsars (with an expected flux density $S \gtrsim 0.1$ mJy at this frequency) we detected 87 pulsars and obtained good quality pulse profiles for most of them. Eight pulsars (B1541+09, B1737+23, B1738–08, B1831–04, B1841–05, B1914+13, B1915+13 and B2111+46) were detected by Seiradakis et al. (1995) but with poor signal-to-noise ratio (S/N) and pulse shapes were not presented. These pulsars were re-observed in the present survey and we obtained good quality profiles in a short integration time. For four other pulsars from our sample (B1900+01, B2016+28, B2045−16, B2310+42), profiles were published by Seiradakis et al. (1995) with poor S/N and are now presented with much better S/N. Eight pulsars which are presented here (B0450−18, B0611+22, B0626−28, B0809+74, B0818−13, B0834+06, B1604−00 and B1818−04), have been observed previously (see Sect. 1) using the old less sensitive system. We observed but did not detect 21 pulsars which are listed in Table 2. From the 33 pulsars not detected by Seiradakis et al. (1995) we attempted to observe 16 pulsars and detected 14 of them. Only two pulsars (B0320+39, B0531+21) were not detected. It is notable that PSR B0320+39 was observed by Kuzmin et al. (1986) at 4.6 GHz but during the last survey (Seiradakis et al. 1995) and in our observations this pulsar was not detected even after 30 min integration time.

The detection limit at 1.4 GHz for the survey by Seiradakis et al. (1995) lies around $S \sim 1$ mJy. The 4.85 GHz survey has yielded a lower limit of $S \sim$ 0.05 mJy, as is visible from Table 1 and the upper limits for not detected pulsars (see Table 2).

Scatter broadening makes it difficult to detect pulsars with high dispersion measure at low frequencies, and only 11 pulsars with dispersion measures $DM > 600$ cm^{-3}pc are known. All of them were discovered at 1.4 GHz (Clifton et al. 1992) or at 1.5 GHz (Johnston et al. 1992). However, scattering is still a limiting factor even at these frequencies. Using the new receiver at 6 cm we detected 9 pulsars with $DM > 500$ cm^{-3}pc. We easily measured, for instance, B1758–23, which has presently the largest known DM of 1074 cm^{-3}pc (see Fig. 1 and Table 1). B1750–24 ($DM = 800$ cm^{-3}pc) shows a double (more likely complex) component profile at 4.85 GHz, whereas the components are completely smeared out at 1.4 GHz due to scatter broadening (Clifton et al. 1992). Finally, we observed four millisecond pulsars at this frequency (for more detailes see Kijak et al. 1997).

In Fig. 1 we present all pulse shapes obtained as result of our observations. The errors in flux density and pulse width were estimated by taking into account the calibration results, the signal-to-noise ratio and the resolution of the profiles. The error of the pulse width after smoothing is indicated by the width of the error box at the lower, right corner of each figure. The results are given in Table 1. For each pulsar, Col. (5) and (6) contain the pulse widths W_{50} and W_{10}. The flux densities S and their errors are listed in Col. (7) and (8), respectively. The spectral index α for flux densities between 1.4 and 4.85 GHz is given in Col. (9) with errors in Col. (10). We assumed that the pulsar flux spectra are well described by a power law of the form $S \propto \nu^{\alpha}$. An index was obtained between 1.4 and 4.85 GHz using data from Lorimer et al. (1995) at 1.4 and 1.6 GHz, Sieber (1973) at 2.7 GHz, Seiradakis et al. (1995) at 1.4 and 4.75 GHz and this paper.

4. Discussion and conclusions

In summary, we present 87 pulse shapes (see Fig. 1), flux densities and pulse width measurements of all detected pulsars in this survey (see Table 1). Up to now we have collected about 130 pulsar profiles at λ 6 cm (see Seiradakis et al. 1995 and this paper). Following a study of pulse shapes (Fig. 1), many pulsar profiles show a complex structure at this high frequency but 23 of them have simple Gaussian shapes. As many as 35 pulsars exhibit no changes at 4.85 GHz as compared to 1.41 GHz. Eight pulsars show slight changes in their shapes as compared to low frequencies while for eight additional sources, the simple profile observed at low frequency is resolved into several components at the high frequency.

The profile width should decrease monotonically with frequency if the emission originates from a magnetospheric region dominated by a dipole magnetic field and a radius-to-frequency mapping exists (Cordes 1978). Considering the profile-width narrowing we constructed a histogram which shows how the pulse width changes between 1.4 GHz and 4.85 GHz (see Fig. 2). For this analysis we used pulse shapes for both frequencies (1.41 and 4.85 GHz) from Seiradakis et al. (1995) and our survey. Figure 2 shows that the pulse widths decrease or in some cases are unchanged with increasing frequency. This effect is also reported by Xilouris et al. (1996). For a few pulsars, pulse widths decreased dramatically. This behaviour is consistent with above assumptions of a hollow-cone model, a radius-to-frequency mapping and a dipolar field structure in the entire emission region.

The increasing pulse width (see Fig. 2) at high frequencies for some pulsars (B0402+61, B0450–18, B0626+24, B0906–17 and B1818–04) is caused by new components appearing in the profile. In Fig. 3, PSR B0906–17 is shown as a typical example. It is seen that the fairly simple profile at low frequency (1.41 GHz) is resolved into a complex one at higher frequency (4.85 GHz), which can be

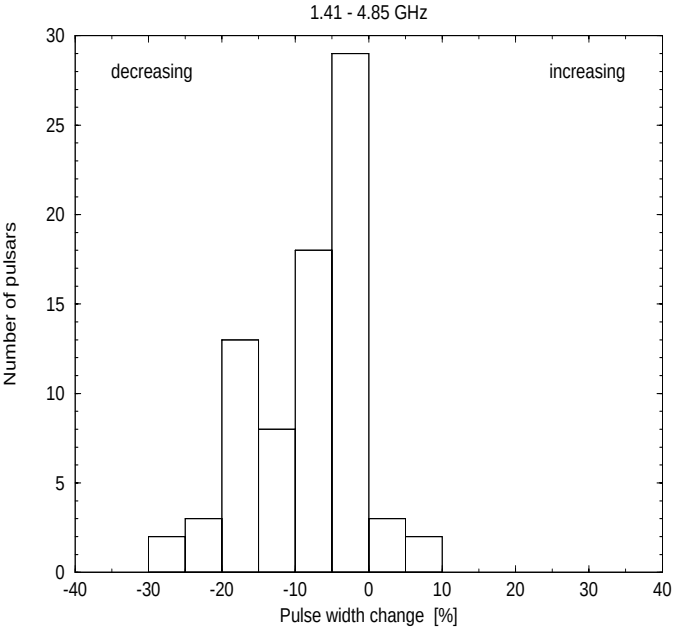

Fig. 2. A distribution of pulse width changes for 78 pulsars. For this analysis we used pulse widths at a level of 10 per cent of the pulse peak

explained geometrically in the context of the multi cone model (Kramer et al. 1994; Sieber 1997). It is obvious that the pulse width and even more the observed pulse shape depend critically on the intensity distribution in the outer parts of the beam. Assuming a semi-Gaussian structure of nested cone beams, the conal emssion (for grazing cuts) becomes more and more dominant as the beam width shrinks at higher frequencies, so that outriders may become visible (see Fig. 3).

Our sample also contains pulsars with very wide profiles. Two pulsars have a pulse width W_{10} larger than 100° (PSR B1831–04 and PSR B1823–13) and five other pulsars have $W_{10} > 70°$ (see Table 1). These pulse widths decrease by less than 10% as compared to 1.4 GHz. Moreover, two pulsars PSR B1702–19 and PSR B1855–09 have been observed with interpulses. Detection of pulsars with interpulses is not very common at high frequencies. Hankins & Fowler (1986) showed that the ratio of interpulse to main pulse intensity decreases considerably with frequency. On the other hand, Wielebinski et al. (1993) have observed an increase of this ratio at the very high frequency of 33.9 GHz for B1929+10. For the millisecond pulsars B1855+09 and J2322+2057 the same behaviour was observed (for more details see Kijak et al. 1997). Up to now we have measured only five pulsars with interpulses at λ 6 cm (B0950+08, B1709–19, B1822-09, B1855+09, B1929+10; Hoensbroech & Xilouris 1997 and this paper).

We have combined the data from this survey with other published flux measurements in the frequency range

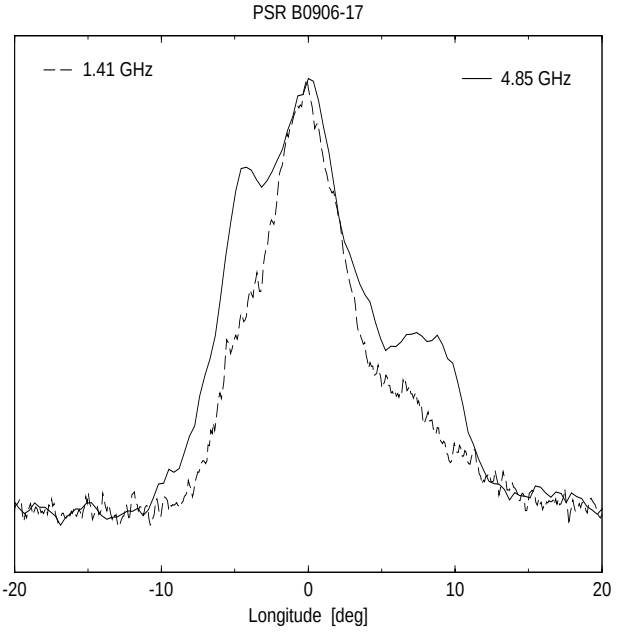

Fig. 3. Pulse shapes of PSR B0906–17 at 1.41 and 4.85 GHz. The development of conal outriders is clearly visible, causing an apparent increase in profile width

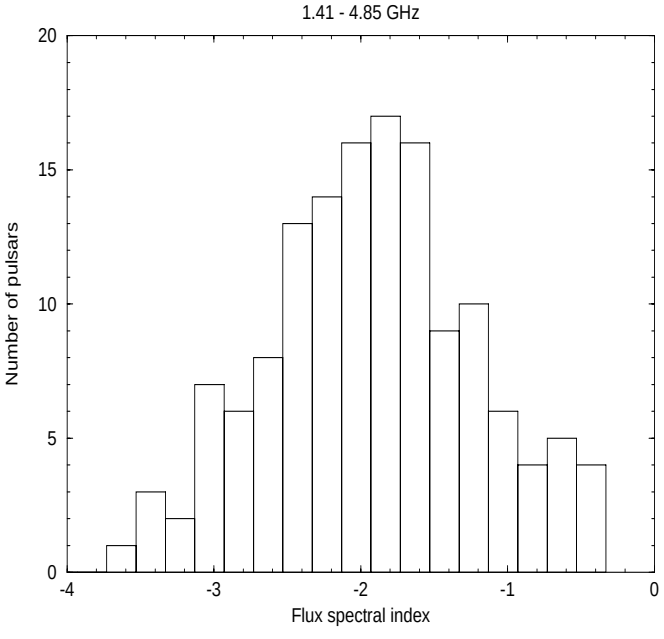

Fig. 4. The distribution of flux spectral index for 141 PSRs

Table 3. Spectral index for several frequency regimes

range of ν (MHz)			α	Reference
1400	-	4850	-1.9	(this paper)
400	-	1600	-1.6	(Lorimer et al. 1995)
160	-	400	-1.2	(Slee et al. 1986)
80	-	160	-0.7	(Slee et al. 1986)

between 1.41 GHz and 4.85 GHz. Figure 4 shows the distribution of spectral indices for all pulsars in the combined sample. This histogram is fairly broad, extending from ~ -3.6 (PSR B0834+06) to ~ -0.4 (PSR B1823−13). The mean spectral index of the sample is -1.9 ± 0.2. The overall distribution of spectral indices is symmetric. In Table 3 we compare the spectral indices for four different frequency regimes. It is cleary seen that the pulsar spectra become steeper at high frequencies.

The main conclusions from this analysis are as follows:

i) The profile shapes do not change much between 1.4 GHz and 4.85 GHz. About 30% of our pulsars have a simple Gaussian shape.

ii) Generally, the pulse widths decrease or are constant at high frequencies (Xilouris et al. 1996 and this paper). This is consistent with the hollow-cone model and the concept of radius-to-frequency mapping (Cordes 1978; Kijak & Gil 1997).

iii) The increasing pulse widths for a few pulsars at higher frequency is consistent with the multi-conal beam structure (Kramer et al. 1994; Sieber 1997).

iv) The flux spectral index α has a mean value of $\sim -1.9 \pm 0.2$, with a symmetric distribution. This result is consistent with previous estimates of the mean spectral index $\bar{\alpha} = -1.8$ (Sieber 1973; Malofeev et al. 1994). In general, pulsars show a steep emission spectrum at 4.85 GHz.

The pulse shapes from our survey and those of Seiradakis et al. (1995) are part of the European Pulsar Network Data Archive, maintained at the Max-Planck-Institut für Radioastronomie in Bonn and are available at: *http://www.mpifr-bonn.mpg.de/pulsar/data/*.

Acknowledgements. We wish to thank O. Lochner and the receiver group for building the excellent 6 cm receiver. We also thank W. Sieber and D. Lorimer for helpful comments. The European Pulsar Network was funded by the European Comission under Human Capital and Mobility grant number CHRX-CT94-0622. This paper is partially supported by the Grant 2 P03D 015 12 of the Polish Committee for Scientific Research (KBN).

References

Backer D.C., Rankin J.M., Campbell D.B., 1976, Nat 263, 202
Clifton T.R., Lyne A.G., Jones A.W., et al., 1992, MNRAS 254, 177
Cordes J., 1978, ApJ 222, 1006
Hankins T.H., Fowler L.A., 1986, ApJ 304, 256
Hoensbroech A.von, Xilouris K.M., 1997, A&AS (in press)

Huguenin G.R., Manchester R.N., Taylor J.H., 1971, ApJ 198, 661
Izvekova V.A., Jessner A., Kuzmin A.D., et al., 1994, A&AS 105, 235
Johnston S., Lyne A.G., Manchester R.N., et al., 1992, MNRAS 255, 401
Gil J., Krawczyk A., 1996, MNRAS 280, 143
Gil J., Krawczyk A., 1997, MNRAS 285, 561
Gil J., Kijak J., Seiradakis J.H., 1993, A&A 272, 268
Kijak J., Gil J., 1997, MNRAS 288, 631
Kijak J., Kramer M., Wielebinski R., Jessner A., 1997, A&A 318, L63
Kramer M., 1994, A&AS 107, 527
Kramer M., Wielebinski R., Jessner A., et al., 1994, A&AS 107, 515
Kramer M., Xilouris K.M., Jessner A., et al., 1996, A&A 306, 867
Kuzmin A.D., Malofeev V.M., Izvekova V.A., et al., 1986, A&A 161, 183
Lorimer D.R., Yates J.A., Lyne A.G., Gould D.M., 1995, MNRAS 273, 411
Lyne A.G., Manchester R.N., 1988, MNRAS 234, 447
Malofeev V.M., Gil J., Jessner A., et al., 1994, A&A 285, 201
Morris D., Graham D., Sieber W., Bartel N., 1981, A&AS 46, 421
Oster L., Sieber W., 1976, A&A 57, 323
Rankin J.M., 1983, ApJ 274, 333
Rankin J.M., 1993, ApJ 405, 285
Ruderman M.A., Sutherland P.G., 1975, ApJ 196, 51
Seiradakis J.H., Gil J., Graham D.A., et al., 1995, A&AS 111, 205
Sieber W., 1973, A&A 28, 237
Sieber W., 1997, A&A 321, 519
Sieber W., Reinecke R., Wielebinski R., 1975, A&A 38, 169
Slee O.B., Alurkar S.K., Bobra A.D., 1986, Aust. J. Phys. 39, 103
Sturrock R.A., 1971, ApJ 164, 529
Wielebinski R., Jessner A., Kramer M., Gil J., 1993, A&A 272, L13
Xilouris K.M., Kramer M., Jessner A., et al., 1996, A&A 309, 481

Table 1. Parameters for detected pulsars at 4.85 GHz. The pulsar name, period, dispersion measure, number of pulses, pulse width at 50%, pulse width at 10%, flux density with error and spectral index with error are listed

PSR B	P (s)	DM ($cm^{-3}pc$)	N (pulses)	W_{50} (deg)	W_{10} (deg)	S (mJy)	σ_S (mJy)	α (1.41 – 4.85 GHz)	σ_α
$0037+56$	1.118	91	1339	3.2	7.7	0.08	0.01	−1.7	0.1
$0053+47$	0.472	18	6293	8.4	13.7	0.06	0.01		
$0138+59$	1.222	35	480	15.8	27.8	0.31	0.03	−2.4	0.1
$0144+59$	0.196	39	4864	3.2	9.5	0.35	0.11	−0.6	0.1
$0301+19$	1.387	16	430	6.0	14.4	0.44	0.05	−2.5	0.2
$0402+61$	0.594	65	1000	5.6	17.2	0.29	0.03	−1.8	0.1
$0450-18$	0.548	40	540	20.0	26.7	0.97	0.10	−1.4	0.1
$0559-05$	0.395	81	4625	11.2	20.0	0.31	0.03	−1.7	0.1
$0609+37$	0.297	27	2000	7.7	13.0	0.11	0.02	−2.1	0.2
$0611+22$	0.334	97	1980	9.5	21.5	0.38	0.04	−1.3	0.1
$0626+24$	0.476	84	4464	14.1	20.0	0.89	0.09	−1.0	0.1
$0628-28$	1.244	34	72	13.7	26.7	9.19	0.90	−0.6	0.2
$0643+80$	1.214	33	1956	3.2	7.4	0.06	0.01	−1.5	0.2
$0751+32$	1.442	39	1160	21.1	24.3	0.15	0.02	−1.4	0.2
$0756-15$	0.682	64	2583	3.9	6.0	0.20	0.02	−1.7	0.1
$0809+74$	1.292	6	693	14.7	29.3	2.45	0.25	−1.3	0.1
$0818-13$	1.238	41	480	6.0	9.8	0.33	0.03	−2.4	0.1
$0834+06$	1.273	13	2772	7.7	10.2	0.07	0.02	−3.5	0.2
$0906-17$	0.401	16	4329	15.1	20.7	0.44	0.05	−1.6	0.2
$0942-13$	0.570	13	4134	6.0	8.4	0.05	0.01	−2.9	0.2
J$1022+10$	0.016	10	138472	8.4	27.0	0.39	0.05	−1.7	0.2
$1039-19$	1.386	32	1210	10.9	15.1	0.55	0.06	−1.1	0.2
$1254-10$	0.617	29	960	8.4	19.0	0.21	0.02	−1.5	0.1
$1541+09$	0.748	35	480	9.5	21.6	0.10	0.01	−3.4	0.1
$1552-23$	0.532	51	2240	6.7	12.3	0.09	0.02	−2.0	0.1
$1604-00$	0.421	11	700	6.5	11.4	1.64	0.16	−0.7	0.2
$1612+07$	1.206	21	1056	1.8	3.2	0.04	0.01	−3.0	0.2
$1620-09$	1.276	70	1067	3.5	7.4	0.05	0.20	−2.0	0.2
$1702-19$	0.298	23	1800	11.6	16.5	1.10	0.11	−1.6	0.3
$1702-19^\star$	0.298	23	1800	4.9	8.8	0.14			
$1709-15$	0.868	58	1003	5.3	9.5	0.08	0.01	−1.8	0.2
J$1713+07$	0.004	16	361020	17.2	82.6	0.80	0.04	−1.7	0.1
$1717-16$	1.565	42	558	3.2	6.3	0.06	0.01	−2.4	0.3
$1737+13$	0.803	49	738	11.3	20.7	0.37	0.04	−1.8	0.1
$1738-08$	2.043	75	287	7.0	14.4	0.14	0.02	−2.1	0.1
$1745-12$	0.394	100	1520	14.8	20.7	1.42	0.14	−0.6	0.1
$1750-24$	0.528	800	1036	17.6	23.7	0.37	0.04	−1.3	0.1
$1753+52$	2.391	35	750	11.6	16.9	0.08	0.01	−2.4	0.2
$1758-23$	0.415	1140	1440	4.9	16.9	0.43	0.04	−2.1	0.1
$1805-20$	0.918	609	1296	9.8	13.0	0.21	0.02	−1.8	0.6
$1815-14$	0.291	595	1020	8.1	17.6	0.51	0.06	−2.1	0.1
$1817-13$	0.921	750	928	4.2	10.6	0.20	0.03	−2.2	0.2
$1818-04$	0.598	84	1000	6.7	14.4	0.43	0.04	−2.4	0.1
$1819-22$	1.874	121	312	8.4	15.1	0.14	0.02	−2.5	0.1
$1820-11$	0.279	428	1431	34.5	51.3	0.64	0.06	−1.4	0.1

Table 1. continued

PSR B	P (s)	DM ($cm^{-3}pc$)	N (pulses)	W_{50} (deg)	W_{10} (deg)	S (mJy)	σ_S (mJy)	α (1.41 – 4.85 GHz)	σ_α
$1821+05$	0.752	67	779	23.2	30.9	0.84	0.09	−1.1	0.1
$1821-11$	0.435	620	6222	3.9	14.4	0.09	0.01	−2.5	0.1
$1822-14$	0.279	360	3392	4.2	8.8	1.20	0.11	−0.7	0.1
$1823-13$	0.101	231	5880	78.0	105.1	2.60	0.26	−0.4	0.1
$1829-08$	0.647	301	920	11.9	23.6	0.15	0.02	−2.8	0.1
$1830-08$	0.085	411	15925	49.9	71.0	0.90	0.08	−1.3	0.1
$1831-04$	0.290	79	2040	126.6	139.9	2.11	0.23	−1.6	0.1
$1839+09$	0.381	49	1560	10.6	13.7	0.22	0.03	−1.6	0.1
$1839+56$	1.652	27	360	6.0	10.9	0.36	0.04	−2.0	0.2
$1841-05$	0.255	400	4698	9.5	19.7	0.32	0.03	−1.7	0.1
$1849+00$	2.180	680	168	22.9	29.5	0.28	0.03	−2.4	0.1
$1855+02$	0.415	504	1584	4.9	14.4	0.51	0.05	−1.1	0.1
$1855+09$	0.005	13	385986	31.6	60.0	1.12	0.09	−1.4	0.2
$1855+09^\star$	0.005	13	385986	14.0	70.0				
$1859+07$	0.644	253	920	10.6	19.7	0.12	0.02	−2.4	0.1
$1900+01$	0.729	246	380	6.7	12.7	0.59	0.06	−1.0	0.2
$1900+06$	0.673	530	1386	2.5	4.6	0.13	0.02	−2.2	0.2
$1905+39$	1.235	30	2004	15.1	23.9	0.17	0.02	−1.9	0.1
$1907+03$	2.330	79	876	50.6	62.3	0.35	0.04	−1.3	0.2
$1911+13$	0.521	144	1708	9.1	17.9	0.15	0.02	−1.7	0.1
$1911-04$	0.825	89	720	6.7	8.8	0.37	0.04	−2.0	0.1
$1913+10$	0.404	246	1480	9.8	16.5	0.15	0.02	−2.3	0.1
$1914+09$	0.270	61	7865	9.8	20.7	0.12	0.01	−1.7	0.1
$1914+13$	0.281	237	8374	6.7	12.0	0.21	0.02	−1.8	0.1
$1915+13$	0.194	95	9240	10.6	17.9	0.16	0.02	−2.7	0.1
$1916+14$	1.181	30	1356	7.0	12.0	0.13	0.01	−1.9	0.3
$1923+04$	1.074	102	945	6.0	8.4	0.16	0.02		
$2000+32$	0.696	135	945	6.7	15.1	0.42	0.04	−0.9	0.1
$2000+40$	0.905	128	656	5.6	16.2	0.13	0.01	−3.0	0.1
$2002+31$	2.111	235	791	10.5	15.8	0.10	0.02	−2.4	0.1
$2011+38$	0.230	239	1040	22.2	39.7	0.72	0.07	−1.9	0.1
$2016+28$	0.557	14	1612	7.9	15.4	0.83	0.09	−3.0	0.2
$2045-16$	1.961	12	602	1.9	13.7	1.05	0.12	−2.8	0.1
$2053+36$	0.221	98	2680	8.4	16.5	0.28	0.03	−1.8	0.1
$2110+27$	1.202	25	1248	3.5	5.3	0.08	0.02	−2.5	0.1
$J2145-07$	0.016	9	112080	12.0	96.0	0.44	0.03	−2.9	0.2
$2111+46$	1.014	141	1764	54.1	69.3	1.89	0.19	−1.9	0.1
$2148+52$	0.332	146	3870	13.0	18.3	0.38	0.04	−1.6	0.1
$2148+63$	0.380	128	3861	9.8	18.3	0.26	0.05	−1.9	0.1
$2154+40$	1.525	71	1125	15.9	22.9	0.57	0.06	−2.8	0.1
$2303+30$	1.575	50	378	4.6	8.1	0.37	0.04	−1.2	0.1
$2310+42$	0.349	17	2646	9.1	14.8	0.50	0.05	−3.0	0.1
$2315+21$	1.222	21	1020	3.2	7.0	0.08	0.01	−2.8	0.2
$2334+61$	0.495	58	1200	15.5	22.2	0.29	0.03	−1.0	0.1

$\star$ - interpulse.

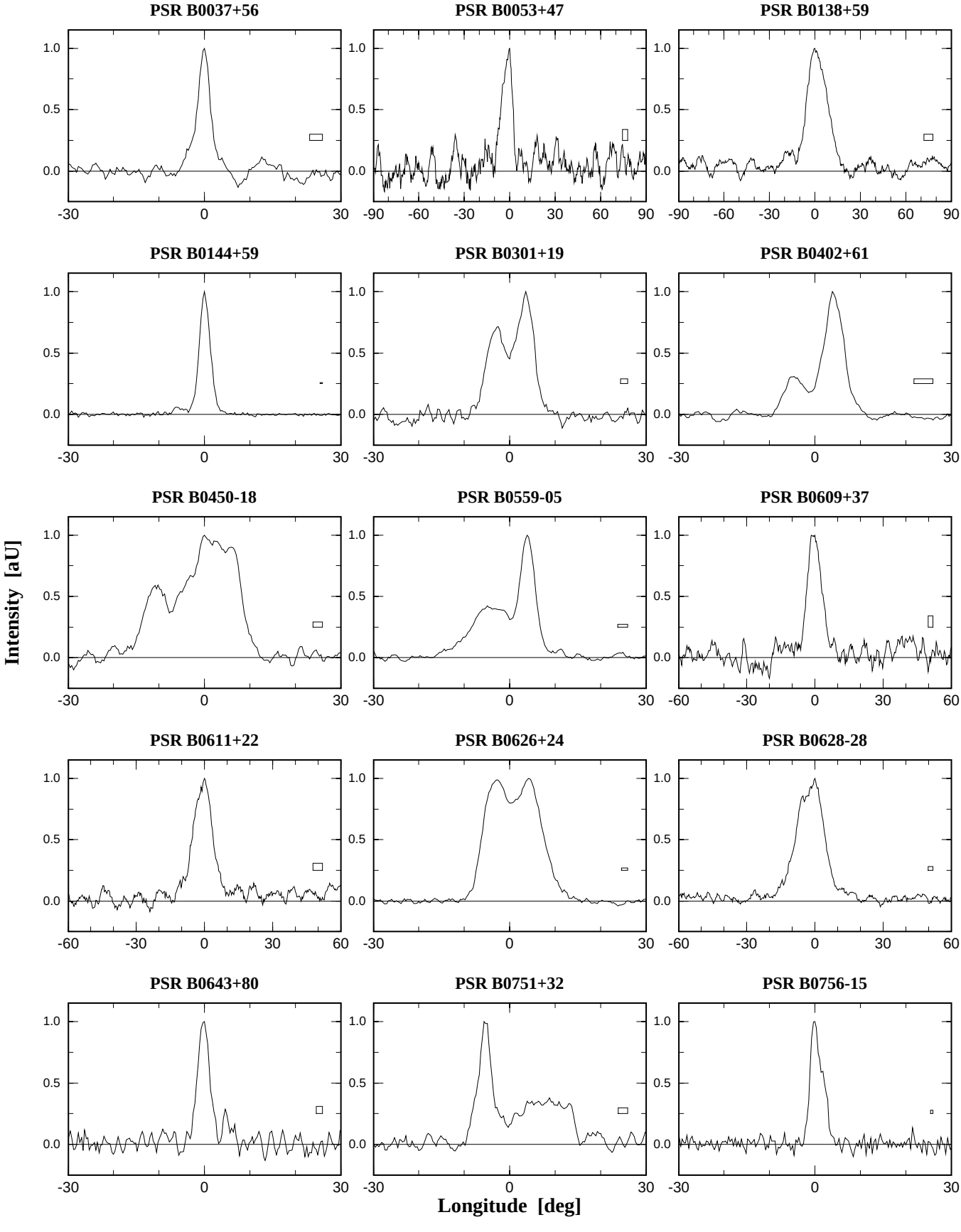

Fig. 1. Pulse shapes for 87 pulsars at 4.85 GHz

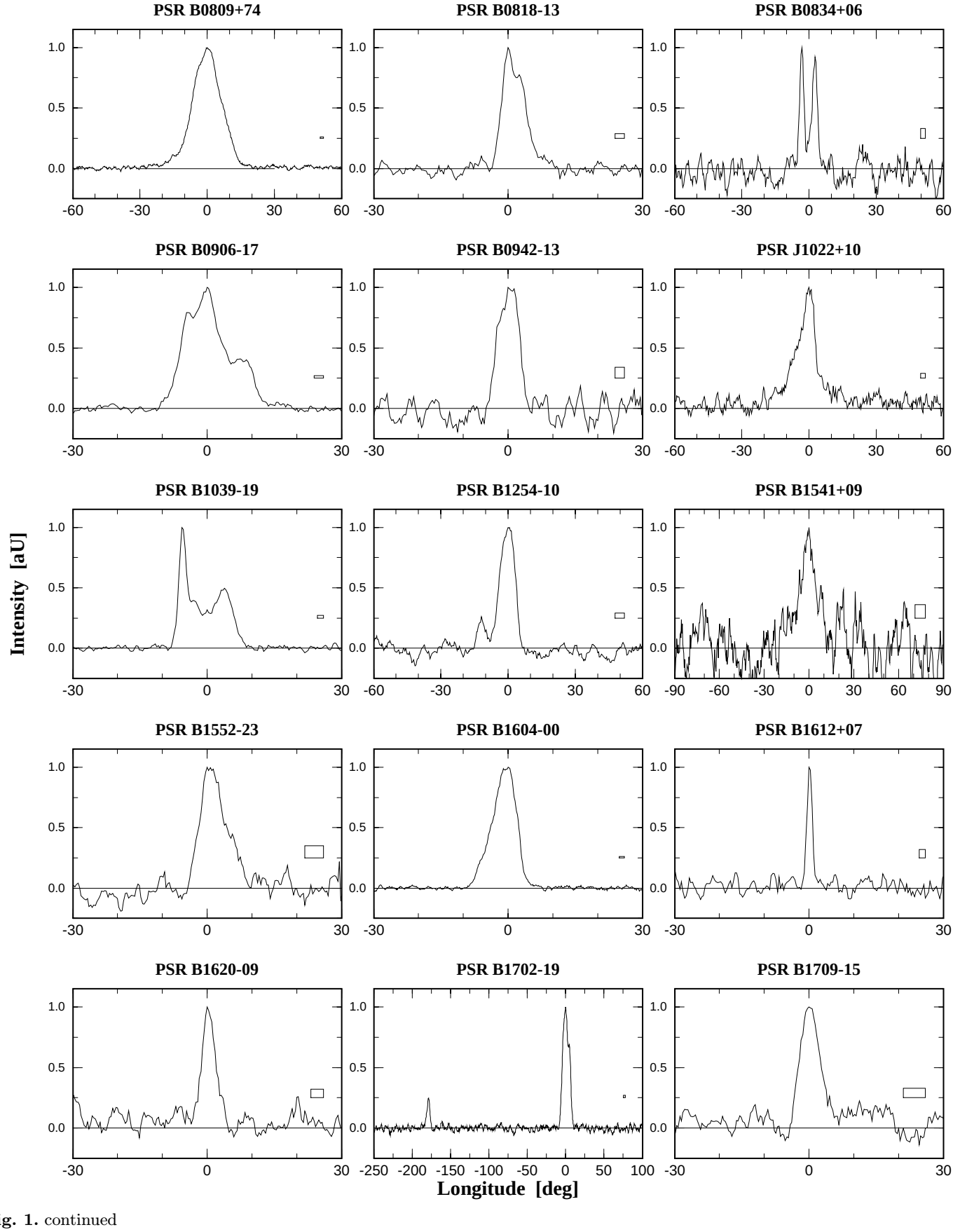

Fig. 1. continued

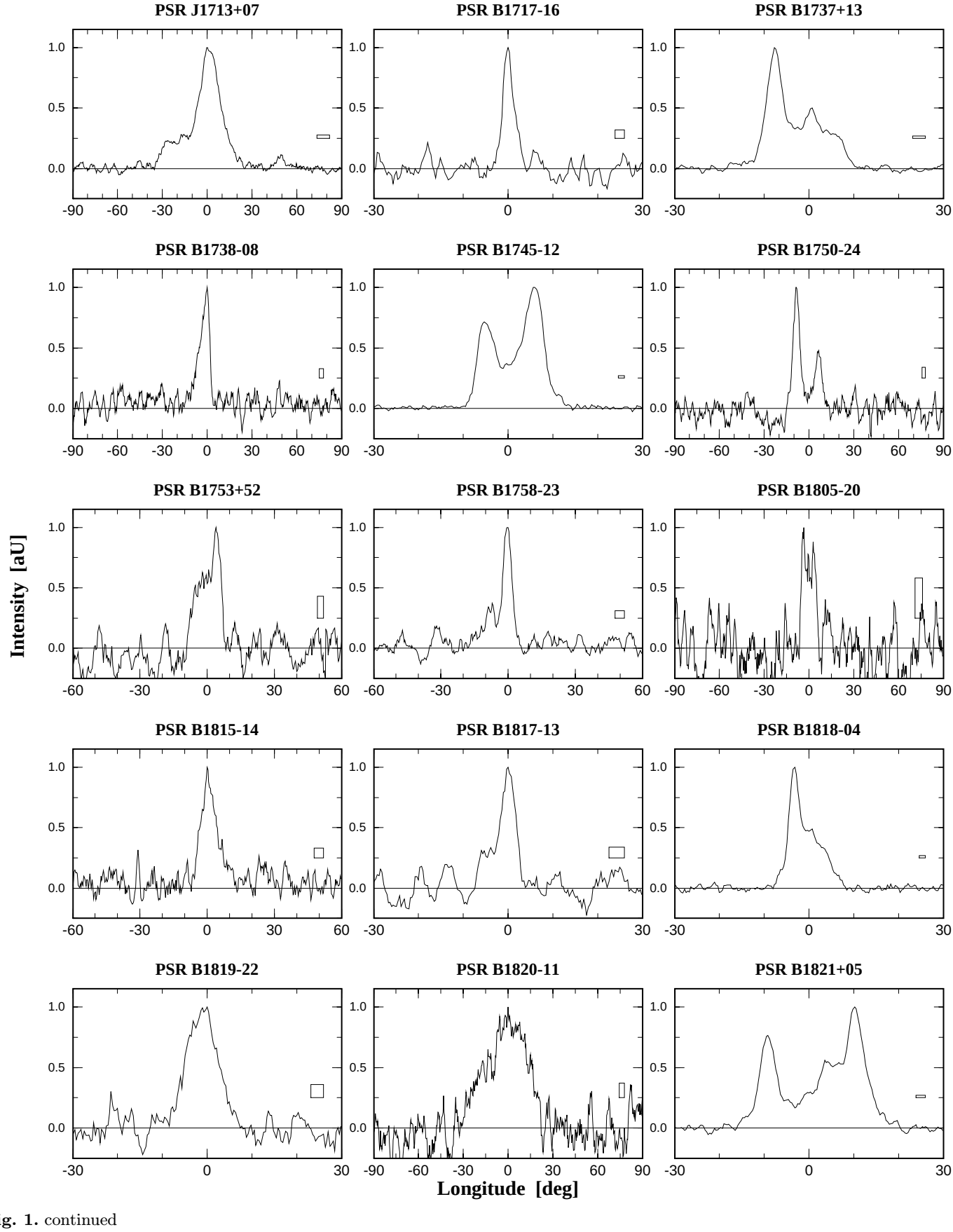

Fig. 1. continued

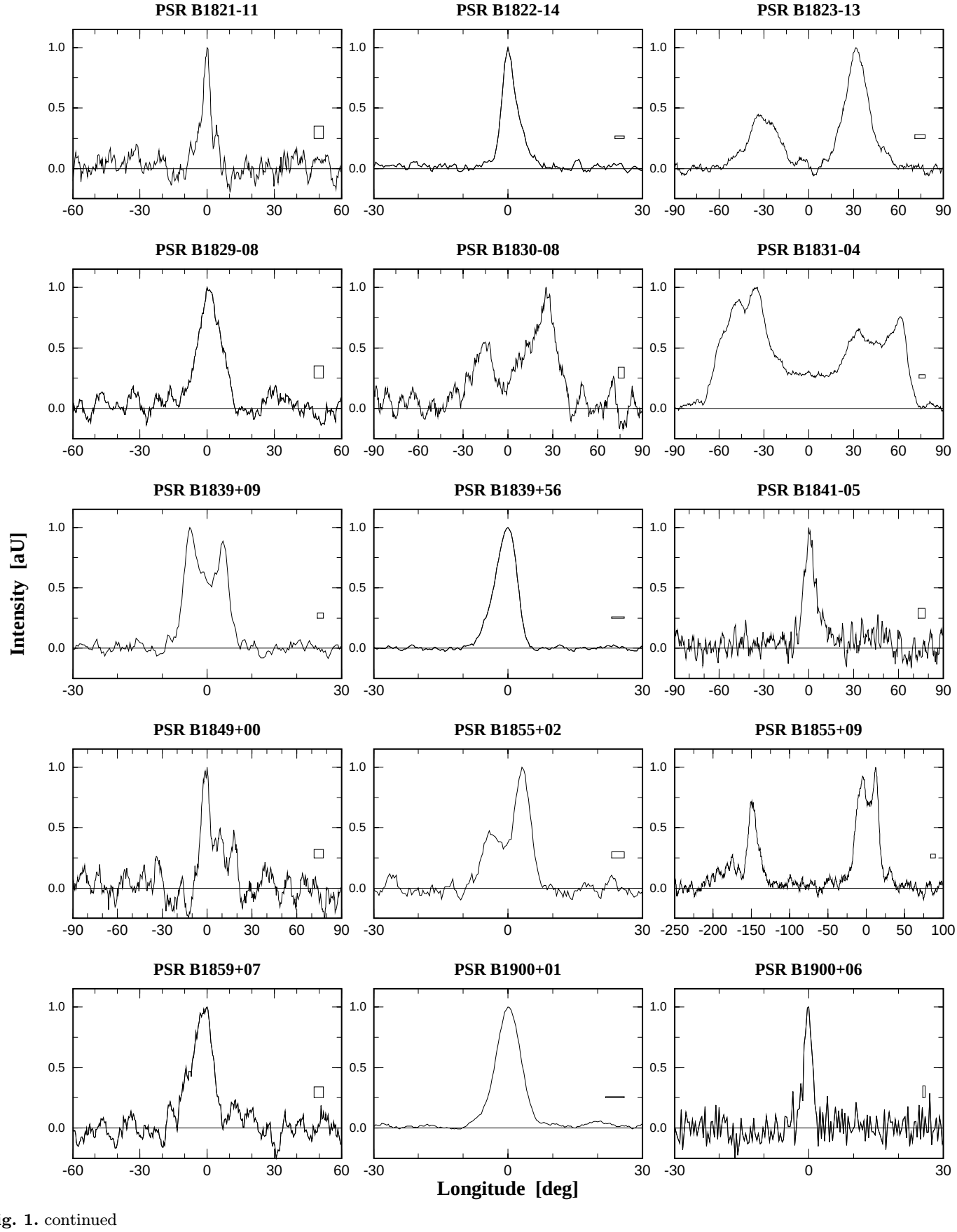

Fig. 1. continued

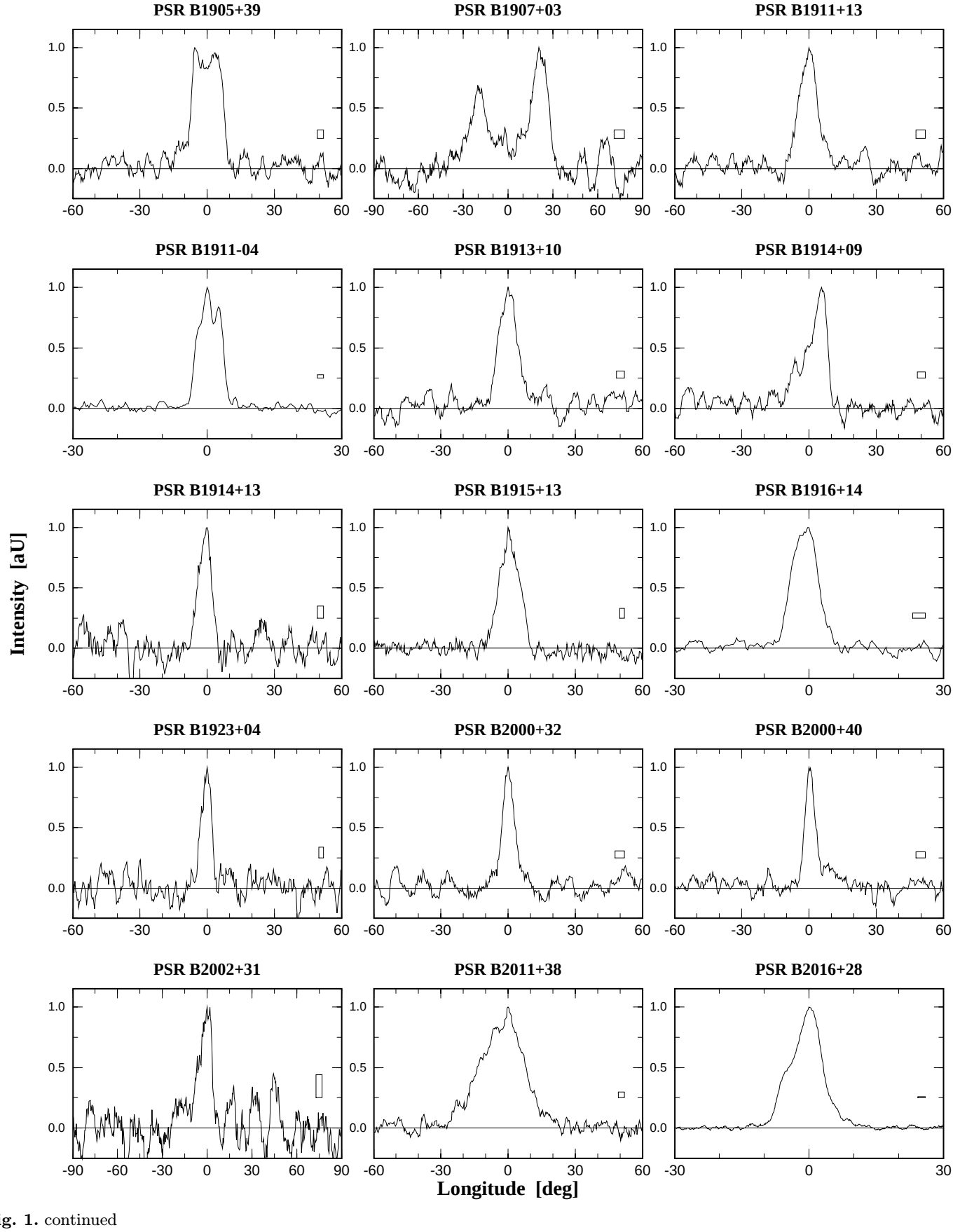

Fig. 1. continued

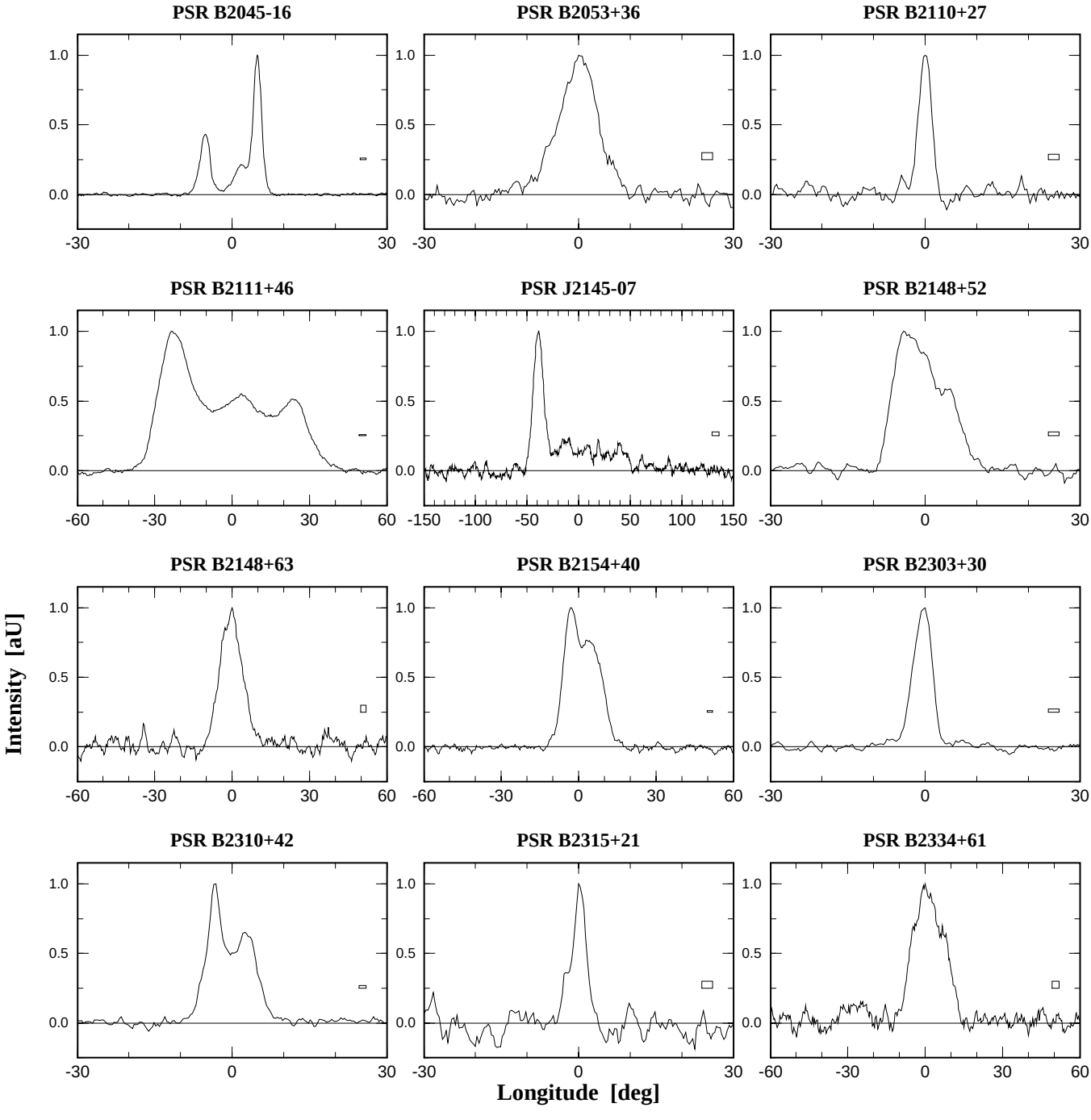

Fig. 1. continued